AIP Advances

A machine learning approach to the prediction of the dispersion property of oxide glass

Cite as: AIP Advances **11**, 125127 (2021); https://doi.org/10.1063/5.0075425
Submitted: 15 October 2021 • Accepted: 05 December 2021 • Published Online: 27 December 2021

Yomei Tokuda, Misa Fujisawa, Jinto Ogawa, et al.

A machine learning approach to the prediction of the dispersion property of oxide glass

Cite as: AIP Advances 11, 125127 (2021); doi: 10.1063/5.0075425
Submitted: 15 October 2021 • Accepted: 5 December 2021 •
Published Online: 27 December 2021

Yomei Tokuda,[1,a)] Misa Fujisawa,[1] Jinto Ogawa,[1] and Yoshikatsu Ueda[2]

AFFILIATIONS

[1] Faculty of Education, Shiga University, Shiga, Japan
[2] Research Institute for Sustainable Humanophere, Kyoto University, Kyoto, Japan

[a)] **Author to whom correspondence should be addressed:** tokuda@edu.shiga-u.ac.jp. **Present address:** Shiga University, 2-5-1, Hiratsu, Otsu City, Shiga Prefecture, Japan.

ABSTRACT

In this study, we built a model for predicting the optical dispersion property of oxide glasses via machine-learning techniques such as kernel ridge regression, neural networks, and random forests. The models precisely predicted the optical property. Based on the predictions for glasses with doped oxides, we prepared new glasses in our laboratory. The experiments agreed well with the predictions made using kernel ridge regression and neural networks but not with those made using random forests. The results of this study demonstrate that the data-driven approach is a promising route for new material design.

INTRODUCTION

Commercial glasses comprise mixtures of oxides that significantly affect their physical properties. Optimized glass composition is essential for the development of new materials having ideal physical characteristics.[1] When creating new materials, we seek low environmental loads and costs. Furthermore, materials used should have targeted properties of chemical durability and physical stability. Therefore, for this study, we explore the desirable properties of glass under several constraints.

Transparent glass is used in optics for cameras, smartphones, and microscopes and is expected to be lightweight and small. Its important properties include refractive index and dispersion. For optical glass, both low dispersion and high refractive indices are required.

The dispersion of glass is described using the Abbe number, as shown in the following equation:[2,3]

$$\nu_d = \frac{n_d - 1}{n_F - n_C}, \tag{1}$$

where n_d, n_F, and n_C are the refractive indices at wavelengths of 587.56, 486.13, and 656.27 nm, respectively. Equation (1) shows that glasses having low dispersion rates have large Abbe numbers and vice versa. Reasonably, a glass with a large Abbe number and a high refractive index is suitable for optics. However, it is well-known that refractive indices and Abbe numbers are roughly traded off;[3] a glass having a high refractive index tends to have a low Abbe number.

Previously, researchers obtained optimized glass mixtures by trial and error,[4,5] and those experimental approaches were often time-consuming. Machine learning is a powerful new method for solving these kinds of problems. In the field of artificial intelligence since the 1960s, machine learning has been employed in the wide field of materials research.[6] To optimize material compositions using machine learning, a model must first be built to estimate the relationship between the glass composition and physical properties. Arguably, the simplest trainable model is that of multiple linear regression (MLR).

Recently, we proposed a glass composition with an improved Abbe number by leveraging kernel ridge regression (KRR),[7] also known as Gaussian process regression (GPR).[7–10] This study demonstrates how the data-driven approach is effective for materials research. KRR is a more complicated model than MLR for predicting precise glass properties because it predicts outputs directly from the input variables without a parametric model. This type of regression is known as non-parametric regression. Other powerful non-parametric regressions are known to be neural networks (NNs)[9,11–14] and random forests (RFs).[15–18] NNs were inspired by theories of the inner workings of biological brains. An outcome is

modeled by a successive set of unobserved variables, called hidden layers, including non-linear or transfer functions.[19] In the case of RFs, different trees can be trained on different subsets of data with randomly chosen subsets of input variables.[19] It is well-known that both non-parametric methods can predict outputs precisely. The purpose of this study is to evaluate the prediction performance of KRRs, NNs, and RFs for the optical production of glass properties and to demonstrate a useful data-driven approach for materials research.

This study proposes a model of the relationship between the glass composition and Abbe number using a KRR, an NN, and an RF. The effects of doped oxides on the Abbe number are also predicted. Glasses are made in the laboratory, and their optical properties are measured. Finally, we validate the prediction power of KRRs, NNs, and RFs by comparing their predicted Abbe numbers with the measured values of glasses prepared using actual doped oxides.

METHOD

Kernel ridge regression (KRR)

KRR is used to model the relationship between glass composition and the Abbe number. It is expressed using a kernel without a parametric model.[8] For elements x_i and x_j corresponding to glass composition, the kernel function, $k(x_i, x_j)$, is defined as the inner product of the characteristic vector, φ, derived from x_i and x_j,[19]

$$k(x_i x_j) = \varphi_m(x_i)^T \varphi_m(x_j) = \sum_{m=1}^{d} \varphi_m(x_i)^T \varphi_m(x_j). \quad (2)$$

An important property of the kernel functions is that the output is expressed as the sum of the weighted kernel functions derived from the inputs.

We can represent $\varphi(x)^T\varphi$ in Eq. (2) by using a radial distribution function to represent k in the following equation:[6]

$$k(x, x') = \alpha^2 \exp\left(\frac{(x - x')^2}{-2\beta^2}\right), \quad (3)$$

where α and β are hyperparameters. This technique is a kernel trick for simplifying complicated calculations.[19]

The output, y^*, is represented as the sum of the kernel function, $k(x, x')$, weighted by parameter, α,

$$y^* = \sum_{i=1}^{N} \alpha_i k(x_i, x). \quad (4)$$

We find parameter α using linear algebra under the condition that x and y_{obs} (instead of y^*) correspond to the glass composition and the reported Abbe number, respectively. The variance and covariance of y^* are a matrix whose elements are kernel functions,

$$K = \begin{pmatrix} k(x_1, x_1) & \cdots & k(x_1, x_N) \\ \vdots & \ddots & \vdots \\ k(x_N, x_1) & \cdots & k(x_N, x_N) \end{pmatrix}, \quad (5)$$

$$k(x, x') = \exp\left(-\sigma(x - x')^2\right). \quad (6)$$

We assume a chained model in which the Gaussian noise, ε, is added to generate the expected y^*, because y^* depends on the input x^*,

$$y^* = k(x^*, x^*)^T (K + \lambda^2 I)^{-1} y_{obs}, \quad (7)$$

where λ is a regularization parameter corresponding to the Gaussian noise. We have now obtained a regression model for the glass composition and Abbe number using KRR.

Neural network (NN)

A multi-layer perceptron is a series of simple perceptrons that model the non-linear relationship between inputs and outputs.[20,21] In a simple perceptron, the linear combination of inputs or predictors is transformed by an activation function, $g(\cdot)$, such as the logistic function

$$h_1(x) = g\left(\beta_{0,1} + \sum_{i=1}^{P} x_j \beta_{j,1}\right), \quad (8)$$

where β is the regression coefficient, $\beta_{j,1}$ is the effect of the jth predictor on the kth hidden unit, and $\beta_{j,0}$ is the bias. In the first layer of the NN, x_j corresponds to the glass composition, as in the case of KRR. Both the number of hidden units and the coefficient, β, will be defined by the regression process. When the hidden units are defined, the stack of the linear combination of the hidden units provides the output,

$$h_{k+1}(x) = g_k\left(\beta_{0,k} + \sum_{i=1}^{P} h_j \beta_{j,k}\right), \quad (9)$$

where $\beta_{0,k}$, $\beta_{j,k}$, and $g_k(\,)$ are the bias, the effect of the jth h_j, and the activation function (i.e., rectified linear unit), respectively. The stack of this layer provides the Abbe number as the output. In addition, a weight decay is included to suppress overfitting, whose formula is similar to λ^2 in Eq. (7).

To train this model, the parameters are optimized to minimize the sum of the residuals. Optimization is a complicated process because there are many parameters to be optimized without constraints.[22] In this study, 56 oxides were identified as predictors. For example, an NN model with five hidden layers requires 342 parameters. A sophisticated back-propagation algorithm is proposed to solve this problem. Back-propagation uses the residuals as derivatives to optimize the parameters in a gradient descent method.[6] All of the above-mentioned parameters, $\beta_{0,k}$ and $\beta_{j,k}$, the number of layers, k, and the weight decay, will be trained.

RF

The decision tree is also effective for regression.[19] The tree model is a successive node that divides the input into two groups, if the input is higher than the threshold. The advantage of the tree model is the interpretability of the results because the division condition can be visualized, whereas overfitting and correlation between the predictors occur easily. To avoid this, a technique known as bagging (i.e., bootstrap aggregation) was proposed.[19] Bagging generates many training datasets by bootstrap-sampling the original data. These datasets are then used to generate a model using the above-mentioned algorithm based on the tree model. Bagging is a simple method with high performance. To improve bagging, RFs were

proposed, where both the data and predictors are randomly selected.[19] As in the case of bagging, the training datasets are prepared by bootstrap sampling. Some of the predictors are chosen for each dataset. In our case, the predictors are chosen from 56 oxides.

Cross Validation (CV)

To estimate precisely, it is important to select parameters α, β, λ, $\beta_{0,k}$, $\beta_{j,k}$, k, and m using CV. For CV, we divide all the data into S sets. (S − 1) sets are chosen as training data for Eq. (4) in the case of KRR. The coefficient of determination, R^2, is evaluated for the remaining data as the test set. The evaluation is repeated S times using a different dataset. The R^2 values obtained from each repetition are averaged to determine the parameters. Here, we selected S = 5 for our data.

Databases

The regression requires glass databases to build models. One commercial database for glass properties is INTERGLAD,[23] which contains ~370 000 glasses and their reported properties. It contains all data from the literature and patents and is updated annually. It is available at the New Glass Forum, Japan.[23] We selected the glass containing SiO_2 as one of its components from INTERGLAD because commercially available glasses contain SiO_2.

Implementation

All codes are written in R.[24,25] The *kernlab*[26] package was used to make the kernel in KRR. The *caret* package was used for the NN and the RF.[27–30] The computation was performed using an Intel Xeon Gold 6226R.

Experimental

One glass with a high refractive index was selected from INTERGLAD with a composition in mol percentage of La_2O_3:Nb_2O_5:Ta_2O_5:GeO_2:B_2O_3:ZrO_2:Al_2O_3:TiO_2:SiO_2:Sb_2O_3 = 21.18:16.94:4.23:13.29:19.36:9.65:5.6:4.83:4.86:0.06. We refer to it as non-doped glass (ND) in this paper. The refractive index and Abbe numbers for ND were reported as 1.9995 and 28.6, respectively.[31] ND is a good starting point because it has a low Abbe number to increase and a high refractive index. Several oxides (CaO, Ga_2O_3, La_2O_3, Nb_2O_5, Sc_2O_3, SrO, Ta_2O_5, Yb_2O_3, etc.) were added to the ND glass at the level of 3 or 5 mol. %. All glass samples were prepared by a melting method using reagent-grade chemicals (FUJIFILM Wako Pure Chemical Corporation). The starting materials were mixed and then melted in a platinum crucible for 1 h at 1400 °C. The melt was subsequently poured onto stainless steel at 300 °C and pressed. The obtained glass was annealed below its transition temperature for 10 min. The glass sample was polished, and then its optical properties were measured as described below.

The refractive indices of the glass plates were measured using a Metricon 2010 prism coupler at wavelengths of 463, 633, 1313, and 1517 nm. The refractive index is approximated by using Cauchy's equation,

$$n = A + \frac{B}{L^2} + \frac{C}{L^4}. \quad (10)$$

Variables A, B, and C were determined, and refractive indices at wavelengths of 486, 587, and 656 nm were predicted. Then, the Abbe number was calculated using Eq. (1).

We compared the reported Abbe number of glasses with that predicted by KRR,[7] NNs, and RFs.

RESULTS AND DISCUSSION

INTERGLAD provides more than 10 000 glasses containing SiO_2 and reports the refractive indices at 587 nm and the Abbe numbers. These glasses contain up to 56 types of oxides as components. A total of 879 glasses with the refractive indices ranging between 1.9 and 2.0 were considered in this study because a high refractive index is desirable for optical glass.

In the case of KRR, the hyperparameters were determined using CV with σ = 0.0001 and λ = 0.0004. We then predicted the Abbe number for the 879 glasses and evaluated the accuracy of the model, as shown in Fig. 1(a). The R^2 was 0.996 for 879 glasses, implying that the regression model has sufficient generalization capability. In the case of NNs, the parameters were determined using CV with k = 17 and weight decay = 0.7. The Abbe number for the 879 glasses and the evaluation of the accuracy of the model are shown in Fig. 1(b). The R^2 value was 0.999 for 879 glasses, which was slightly greater than that of KRR. RFs also predicted the Abbe number for the 879 glasses, and the evaluation of the accuracy of the model is shown in Fig. 1(c). The R^2 value was 0.996. The best number of predictors for the RF was 30. These R^2 values show that all methods showed highly accurate predictions for the reported glasses.

As noted above, the glasses we selected contain 56 types of oxides. The purpose of this study was to find the oxides that increase the Abbe number by means of machine learning. We will explain how to dope the oxide by using La_2O_3 as an example. We added 5 mol. % La_2O_3 to the ND glass, changing the sum of composition percentages from 100 to 105 mol. %. The percentage of each oxide in the doped glass was then multiplied by 100/105. This procedure ensured that a glass with compositions equaling 100 mol. % was obtained. Then, the Abbe number was predicted using Eq. (7). This calculation predicted the extent to which the addition of the new component of 5 mol. % La_2O_3 affected the Abbe number. The predicted Abbe numbers for the glass with doped oxides are listed for a doping level of 3% in Table I and 5% in Table II. The predicted data for all the glasses with doped oxides are also listed in supplementary material Table S1. The measured value of ND glass was smaller than the reported one. Accordingly, we consider the difference between the predicted and measured Abbe numbers for the ND and doped glasses. These values are also tabulated in Tables I and II.

As listed, the ten components predicted by means of KRR to increase the Abbe number most strongly were Yb_2O_3, followed by CaO, Na_2O, Ga_2O_3, GeO_2, BaO, Li_2O, Gd_2O_3, La_2O_3, and ZrO_2. On the other hand, the decrement oxides were Nb_2O_5 and Ta_2O_5. In the case of NNs, the top-ten oxides that increased the Abbe number were Yb_2O_3, La_2O_3, CaO, Gd_2O_3, Lu_2O_3, GeO_2, SiO_2, B_2O_3, SrO, and P_2O_5, whereas those decreasing it were In_2O_3 and Sc_2O_3. RFs show the top-10 oxides with increasing Abbe numbers: SiO_2, La_2O_3, Y_2O_3, Gd_2O_3, GeO_2, Ta_2O_5, TiO_2, Yb_2O_3, Sb_2O_3, and WO_3. Those decreasing included ZrO_2 and Bi_2O_3.

To validate these predictions, we selected doped oxides of CaO, Ga_2O_3, GeO_2, La_2O_3, Nb_2O_5, Sc_2O_3, SrO, Ta_2O_5, TeO_2, TiO_2, Y_2O_3,

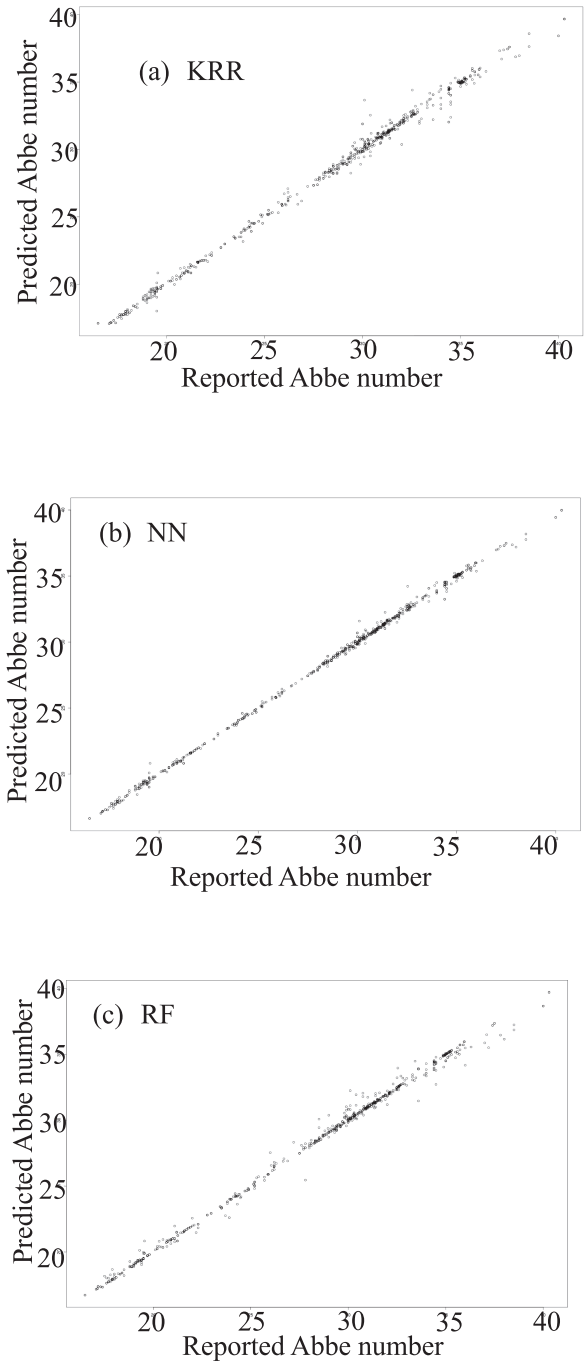

FIG. 1. Predicted Abbe number plotted against the reported Abbe number for (a) KRR, (b) NN, and (c) RF.

and Yb_2O_3 at doping levels of 3% and 5% in consideration of vitrification. The Abbe numbers for the doped glasses are listed in Tables I and II. The mark "–" in Table II means that the glass could not be obtained. At a doping level of 3%, the linear regression equations of the predicted values against the measured values for KRR, NNs, and RFs were y = −0.23x + 35.02, y = −1.78x + 75.127, and y = 19.4x −528.3, respectively, as shown in Fig. 2. This result indicates disagreement between the predictions and measurements. This disagreement may follow a change in composition that occurs during melting because the raw materials tend to be volatile at high temperatures. For a dopant level of 5%, the linear regression equations for KRR, NNs, and RFs were y = 0.70x + 9.75, y = 0.44x + 16.62, and

TABLE I. The predicted and measured values of Abbe number. The first column is the dopant at a doping level of 3%, and ND indicates the non-doped glass. The second, third, and fourth columns show the predicted values by means of KRR, NNs, and RFs, respectively. The fifth, sixth, and seventh columns show the difference in the predicted Abbe number between the doped and non-doped glass. The term exp and Δexp mean the measured value and the difference in the measured Abbe number between the doped and non-doped glass, respectively.

	KRR[a]	NN	RF	ΔKRR	ΔNN	ΔRF	Exp.	Δexp
CaO	29.4	29.0	28.5	0.9	0.5	0.0		
Ga_2O_3	29.2	26.8	28.5	0.7	−1.7	0.0	25.7	−0.5
GeO_2	29.2	28.8	28.5	0.7	0.3	0.0	25.9	−0.3
La_2O_3	29.0	29.1	28.9	0.5	0.6	0.4		
Nb_2O_5	27.4	27.7	28.4	−1.1	−0.8	−0.1		
Sc_2O_3	28.2	21.0	28.5	−0.3	−7.5	0.0	29.6	3.4
SrO	28.8	28.6	28.5	0.3	0.1	0.0		
Ta_2O_5	27.1	27.4	28.3	−1.4	−1.1	−0.2		
TeO_2	28.5	28.2	28.4	0.0	−0.3	−0.1	26.8	0.6
TiO_2	28.6	28.5	28.5	0.1	0.0	0.0	26.8	0.6
Y_2O_3	28.9	28.2	29.0	0.4	−0.3	0.5	26.1	−0.1
Yb_2O_3	29.7	29.1	28.5	1.2	0.6	0.0	27.1	0.9
ND	28.6	28.5	28.5				26.2	

[a]The data were taken from our previous work.[7]

TABLE II. The predicted and measured values of Abbe number. The first column is the dopant at a doping level of 5%, and ND indicates the non-doped glass. The second, third, and fourth columns are the predicted values by means of KRR, NNs, and RFs, respectively. The fifth, sixth, and seventh columns are the difference in the predicted Abbe number between the doped and non-doped glass. The term exp and Δexp mean the measured value and the difference in the measured Abbe number between the doped and non-doped glass, respectively.

	KRR[a]	NN	RF	ΔKRR	ΔNN	ΔRF	Exp.	Δexp
CaO	30.0	29.2	28.0	1.5	0.7	−0.5	26.9	0.7
Ga_2O_3	29.7	25.3	28.0	1.2	−3.2	−0.5	27.4	1.2
GeO_2	29.6	29.0	28.2	1.1	0.5	−0.3		
La_2O_3	29.4	29.4	28.6	0.9	0.9	0.1	29.4	3.2
Nb_2O_5	26.7	27.2	27.9	−1.8	−1.3	−0.6	24.3	−1.9
Sc_2O_3	28.0	19.0	28.0	−0.5	−9.5	−0.5		
SrO	28.9	28.8	28.0	0.4	0.3	−0.5	27.0	0.8
Ta_2O_5	26.3	26.3	28.1	−2.2	−2.2	−0.4	25.7	−0.5
TeO_2	28.4	28.0	28.0	−0.1	−0.5	−0.5		
TiO_2	28.6	28.5	28.0	0.1	0.0	−0.5		
Y_2O_3	29.1	28.0	28.5	0.6	−0.5	0.0		
Yb_2O_3	30.4	29.4	28.1	1.9	0.9	−0.4		
ND	28.6	28.5	28.5				26.2	

[a]The data were taken from our previous work.[7]

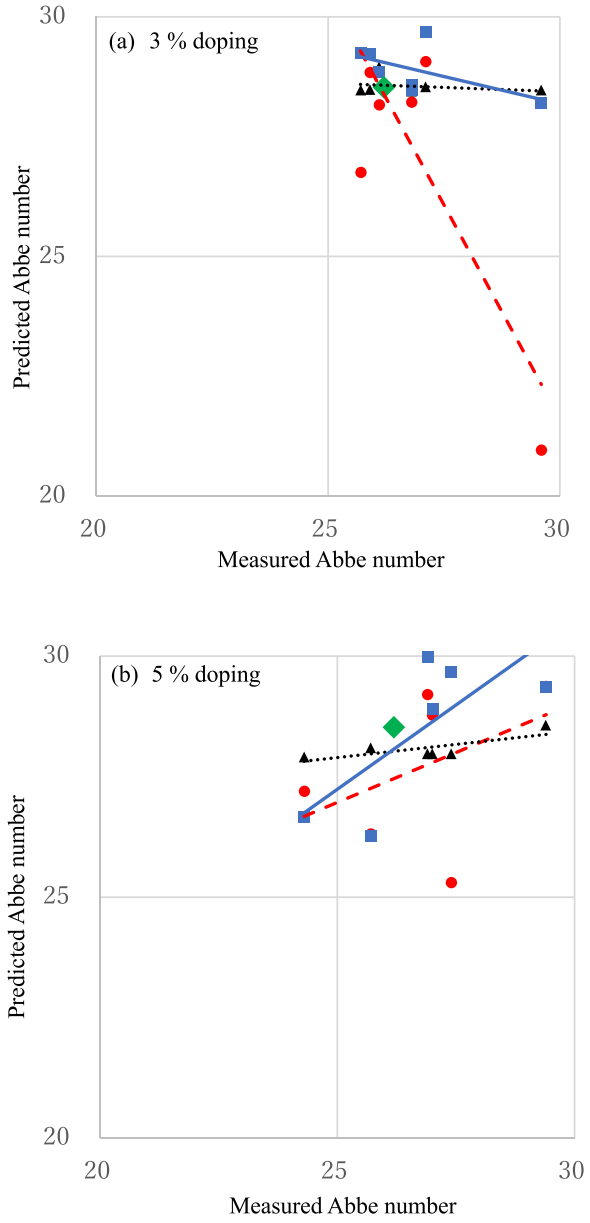

FIG. 2. Measured and predicted Abbe number for doping level of (a) 3% and (b) 5%. The blue square, red circle, black triangle, and green diamond corresponds to KRR, NN and RF, ND glass, respectively. The linear regression lines are also shown as blue straight line for KRR, red dashed line for NN and black dotted line for RF.

$y = 0.11x + 25.16$, respectively, as shown in Fig. 2. This result shows that the performance of KRR was better than that of NNs and can predict the Abbe number of the doped glass whereas RFs is not suitable for predicting the Abbe number.

In the following, we focused on KRR and NNs. In line with the prediction by KRR and NNs, the experiment showed that doping with CaO, GeO_2, La_2O_3, SrO, and Yb_2O_3 increased the Abbe number whereas Nb_2O_5, Sc_2O_3, Ta_2O_5, and TeO_2 decreased it. These trends without Sc_2O_3 are consistent with the measured values (Tables I and II). Therefore, KRR and NNs are useful for predicting the dispersion of the oxide glasses. Sc_2O_3 is noted because the Abbe number was predicted to decrease both in the case of KRR and largely in the case of NNs, whereas the measured value increased by +3.4 at a doping level of 3%, indicating the inaccurate prediction. We believe that this is because there was only one datum that included Sc_2O_3 in the 879 training data.

These results demonstrate the effectiveness of the machine-learning approach, especially KRR and NNs, for creating new materials with no guidance or intuitive reasoning. Prediction using machine learning provided the next guess, which was the oxide used for doping for increasing the Abbe number. These results also demonstrated that the data-driven approach is a potential advantage to materials research.

CONCLUSIONS

Machine learning for materials research presents great challenges. To address this, KRR, NN, and RF machine-learning methods were used for predicting glass properties with no guidance or intuitive reasoning. The method succeeded in accurately learning the relationship between optical properties and glass composition. We also predicted the optical properties of glasses with their dopants and tested them experimentally by means of KRR and NNs. There was good agreement, especially when using the KRR between the predicted and experimental values. Therefore, this work is a successful demonstration of machine learning for material design and can be used for developing new inorganic materials.

SUPPLEMENTARY MATERIAL

See the supplementary material for the Abbe number estimated by KRR, NNs, and RFs for all the oxides, which are tabulated in Table S1.

ACKNOWLEDGMENTS

This study was partially supported by the Asahi Glass Foundation and Shiga University. The optical experiment was carried out on a Metricon 2010 prism coupler at Osaka Prefecture University (Professor M. Takahashi). We are grateful to Dr. Daniel M. Packwood for helpful discussions.

AUTHOR DECLARATIONS

Conflict of Interest

The authors declare no conflicts of interest.

Author Contributions

Y.T. contributed toward conceptualization, software, writing the original draft, and supervision; M.F. contributed toward investigation and software; J.O. contributed toward investigation; and Y.U. contributed toward validation and investigation.

DATA AVAILABILITY

The data that support the findings of this study are available from the corresponding author upon reasonable request.

REFERENCES

[1] F. Gan, J. Non-Cryst. Solids **184**, 9 (1995).
[2] J. E. Shelby, *Introduction to Glass Science and Technology* (Royal Society of Chemistry, 2005).
[3] P. Hartmann, R. Jedamzik, S. Reichel, and B. Schreder, Appl. Opt. **49**, D157 (2010).
[4] J. Chung, Y. Watanabe, Y. Yananba, Y. Nakatsuka, and H. Inoue, J. Am. Ceram. Soc. **103**, 167 (2020).
[5] S. Fujino, H. Takebe, and K. Morinaga, J. Am. Ceram. Soc. **78**, 1179 (1995).
[6] C. M. Bishop, *Pattern Recognition and Machine Learning* (Springer, 2006).
[7] Y. Tokuda, M. Fujisawa, D. M. Packwood, M. Kambayashi, and Y. Ueda, AIP Adv. **10**, 105110 (2020).
[8] C. K. I. Rasmussen and C. Williams, *Gaussian Processes for Machine Learning* (MIT Press, 2006).
[9] S. Bishnoi, S. Singh, R. Ravinder, M. Bauchy, N. N. Gosvami, H. Kodamana, and N. M. A. Krishnan, J. Non-Cryst. Solids **524**, 119643 (2019).
[10] S. Bishnoi, R. Ravinder, H. S. Grover, H. Kodamana, and N. M. A. Krishnan, Mater. Adv. **2**, 477 (2021).
[11] D. R. Cassar, Acta Mater. **206**, 116602 (2021).
[12] D. S. Brauer, C. Rüssel, and J. Kraft, J. Non-Cryst. Solids **353**, 263 (2007).
[13] R. Ravinder, K. H. Sridhara, S. Bishnoi, H. S. Grover, M. Bauchy, and Jayadeva, Mater. Horizons **7**, 1819–1827 (2020).
[14] C. Dreyfus and G. Dreyfus, J. Non-Cryst. Solids **318**, 63 (2003).
[15] H. Liu, Z. Fu, K. Yang, X. Xu, and M. Bauchy, J. Non-Cryst. Solids **4**, 100036 (2019).
[16] E. Alcobaça, S. M. Mastelini, T. Botari, B. A. Pimentel, D. R. Cassar, A. C. P. d. L. F. de Carvalho, and E. D. Zanotto, Acta Mater. **188**, 92 (2020).
[17] B. Deng and Y. Zhang, Chem. Phys. **538**, 110898 (2020).
[18] B. Deng, J. Non-Cryst. Solids **529**, 119768 (2020).
[19] K. P. Murphy, *Machine Learning: A Probabilistic Perspective* (MIT Press, 2012).
[20] G. James, D. Witten, T. Hastie, and R. Tibshirani, *An Introduction to Statistical Learning* (Springer, 2013).
[21] T. Hastie, R. Tibshirani, and J. Friedman, *The Elements of Statistical Learning* (Springer, 2003).
[22] M. Kuhn and K. Johnson, *Applied Predictive Modeling* (Springer, 2016).
[23] New Glass Forum, https://www.newglass.jp, 1991.
[24] RCoreTeam, https://www.r-project.org, 2019.
[25] RStudioTeam, http://www.rstudio.com/, 2020.
[26] A. Alexandros, A. Smola, and K. Hornik, J. Stat. Software **11**, 1 (2004).
[27] M. Kuhn, J. Wing, S. Weston, A. Williams, C. Keefer, A. Engelhardt, T. Cooper, Z. Mayer, B. Kenkel, R. C. Team, and M. Benesty, https://cran.r-project.org/web/packages/caret/index.html, 2021.
[28] M. Kuhn and K. Johnson, *Applied Predictive Modeling* (Springer, 2016).
[29] W. N. Venebles and B. D. Ripley, *Modern Applied Statistics with S* (Springer, 2002).
[30] L. Breiman, Mach. Learn. **45**, 5 (2001).
[31] Ohara Inc., Japanese Unexamined Patent Application Publication No. 2009-203155 (10 September 2009).